International Journal of Mass Spectrometry 309 (2012) 70–78

Contents lists available at SciVerse ScienceDirect

International Journal of Mass Spectrometry

journal homepage: www.elsevier.com/locate/ijms

Knudsen effusion mass spectrometric approach to the thermodynamics of Na_2O–Nb_2O_5 system

A. Popovič[a,*], L. Bencze[b], J. Koruza[a], B. Malič[a], M. Kosec[a]

[a] Jozef Stefan Institute, Jamova 39, SI-1000 Ljubljana, Slovenia
[b] Eötvös Loránd University, Department of Physical Chemistry, H-1117 Budapest, Pázmány Péter sétány 1/A, Hungary

ARTICLE INFO

Article history:
Received 25 May 2011
Received in revised form 23 August 2011
Accepted 29 August 2011
Available online 3 September 2011

Keywords:
Knudsen cell
Activity
Gibbs energy
Sodium niobates
Evaporation
Sodium oxide

ABSTRACT

Knudsen effusion mass spectrometry (KEMS) was used to determine the equilibrium vapour pressures of sodium over five selected compositions in different solid two-phase regions of the Na_2O–Nb_2O_5 system at 1100–1470 K. The results were then used to determine the standard thermodynamic functions ($\Delta_f G_T^\circ$, $\Delta_f H_{298\,K}^\circ$, S_T°) of five solid compounds: Na_3NbO_4, $NaNbO_3$, $Na_2Nb_4O_{11}$, $NaNb_3O_8$ and $NaNb_{13}O_{33}$. These data were then incorporated into the IVTANTHERMO database to perform equilibrium calculations under real conditions relevant to the high temperature stability of sodium niobate, which is an important end member of the alkali niobate-based lead-free piezoelectric ceramics.

1. Introduction

Lead-based perovskite ceramics like $Pb(Zr,Ti)O_3$ and $Pb(Mg_{1/3}Nb_{2/3})O_3$–$PbTiO_3$ are widely used in piezoelectric applications, such as sensors, actuators and transducers. Since the lead content in these materials is usually more than 60 wt.% a great deal of research is focused on finding environmentally friendly alternatives (Rödel et al. [1]). One promising group of lead-free materials is based on alkaline niobates (Shrout and Zhang [2], Malič et al. [3], Rödel et al. [1]), with some compositions already exhibiting piezoelectric properties comparable to the lead-based perovskites (Saito et al. [4]).

In spite of their potential little has been done experimentally to investigate the thermo-chemistry of the basic systems for these materials, such as the sodium oxide (Na_2O)–diniobium pentoxide (Nb_2O_5) system. Despite this Sue [5] has performed a series of manometric measurements of the equilibrium reactions

$$Nb_2O_5 + Na_2CO_3 \Leftrightarrow 2NaNbO_3 + CO_2 \quad (1)$$

$$NaNbO_3 + Na_2CO_3 \Leftrightarrow Na_3NbO_4 + CO_2 \quad (2)$$

to obtain thermo-chemical information (heat of formation from the elements) for the two sodium niobate phases. More recently, Näfe et al. [6] employed Sue's original pressure data for reactions (1) and (2) to determine the difference in the standard Gibbs energies of formation of the two-niobate phases. Amin [7] also undertook an extensive experimental study of the Na_2O–Nb_2O_5 system using electrochemical methods in his PhD Thesis. A part of his results was published by Näfe et al. [6], where again, only the difference in the standard Gibbs energies ($\Delta_f G_T^\circ$) was obtained as a function of temperature [6,7]. The standard heat of formation of $NaNbO_3$(s) from oxides was measured by Pozdnyakova and Navrotsky [8] using drop solution calorimetry and more recently by Xu et al. [9] using the same technique. The standard heat of formation of $NaNbO_3$ from elements was calculated by Shigemi and Wada [10] using the first principle calculation, which was also assessed by Vaskresenskaya and Budova [11]. To our knowledge, these studies represent the experimental thermodynamical data available for compounds in the Na_2O–Nb_2O_5 system. Lindemer et al. [12] reported the estimated values of standard entropies and enthalpies of formation of the above-mentioned compounds to be in agreement (about 90%) with values estimated by Yungman [13]. In addition to Na_3NbO_4 and $NaNbO_3$ other solid phase compounds for example $Na_2Nb_4O_{11}$, $NaNb_3O_8$ and $NaNb_{13}O_{33}$, have been identified in this system by various authors for which thermodynamical functions have yet to be determined. The aim of this study is therefore to obtain a better understanding of the thermodynamics of this system by measuring the vapour pressure over the equilibrium Na_2O–Nb_2O_5 solid mixtures at five pre-selected compositions using Knudsen effusion mass spectrometry (KEMS). This method is known as one of the most powerful ones as far as determining Gibbs energy is concerned.

* Corresponding author. Tel.: +386 1 4773490; fax: +386 1 251 93 85.
E-mail address: arkadij.popovic@ijs.si (A. Popovič).

1387-3806/$ – see front matter © 2011 Elsevier B.V. All rights reserved.
doi:10.1016/j.ijms.2011.08.028

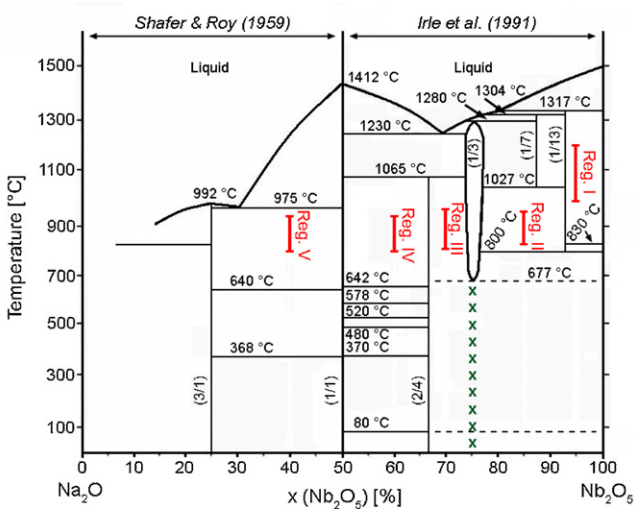

Fig. 1. A Na_2O–Nb_2O_5 phase diagram combined from Shafer and Roy [14] and Irle et al. [15]. Five compositions and temperature ranges of measurements are indicated by vertical bars. Note that according to X-ray results phase $NaNb_3O_8$ is present upon cooling to room temperature (marked with ×).

1.1. Thermodynamic background

To obtain the standard Gibbs energies of formation of the individual sodium niobate compounds it is necessary to perform Na_2O activity measurements within all two-phase regions of the system, starting from Nb_2O_5 as far as the Na_2O side of phase diagram. According to the phase diagram, constructed from the studies of Shafer and Roy [14] and Irle et al. [15], the $NaNb_{13}O_{33}(s)$ phase coexists at 900 °C with $Nb_2O_5(s)$ (Fig. 1, region I).

The evaporation of Na_2O within this region (region I) is incongruent (composition of solid and vapour phase differ) and described by the equilibrium evaporation reaction (3) as follows:

$$2NaNb_{13}O_{33}(s) \Leftrightarrow 13Nb_2O_5(s) + Na_2O(g) \quad (3)$$

and the corresponding standard solid phase decomposition reaction:

$$2NaNb_{13}O_{33}(s) = 13Nb_2O_5(s) + Na_2O(s) \quad (4)$$

Gibbs energy of reaction (4) is then

$$\begin{aligned}\Delta_r G^\circ(4) &= -RT\ln(a_{Na_2O}(I)) \\ &= \Delta_f G^\circ(Na_2O(s)) + 13\Delta_f G^\circ(Nb_2O_5(s)) \\ &\quad - 2\Delta_f G^\circ(NaNb_{13}O_{33}(s)) \end{aligned} \quad (5)$$

It follows from Eq. (5) that the Gibbs energy of formation of $NaNb_{13}O_{33}(s)$ is

$$\begin{aligned}&\Delta_f G^\circ(NaNb_{13}O_{33}(s)) \\ &= \frac{1}{2}[\Delta_f G^\circ(Na_2O(s)) + 13\Delta_f G^\circ(Nb_2O_5(s)) + RT\ln(a_{Na_2O}(I))] \end{aligned} \quad (6)$$

By knowing $\Delta_f G^\circ(NaNb_{13}O_{33}(s))$ one can obtain $\Delta_f G^\circ$ for $NaNb_3O_8(s)$, $Na_2Nb_4O_{11}(s)$, $NaNbO_3(s)$ and $Na_3NbO_4(s)$ as follows:

$$\begin{aligned}\Delta_f G^\circ(NaNb_3O_8(s)) = \frac{5}{13}\Big[&\Delta_f G^\circ(Na_2O(s)) + \frac{3}{5}\Delta_f G^\circ(NaNb_{13}O_{33}(s)) \\ &+ RT\ln(a_{Na_2O}(II))\Big] \end{aligned} \quad (7)$$

$$\begin{aligned}\Delta_f G^\circ(Na_2Nb_4O_{11}(s)) = \frac{1}{3}[&\Delta_f G^\circ(Na_2O(s)) + 4\Delta_f G^\circ(NaNb_3O_8(s)) \\ &+ RT\ln(a_{Na_2O}(III))] \end{aligned} \quad (8)$$

$$\begin{aligned}\Delta_f G^\circ(NaNbO_3(s)) = \frac{1}{4}[&\Delta_f G^\circ(Na_2O(s)) + \Delta_f G^\circ(Na_2Nb_4O_{11}(s)) \\ &+ RT\ln(a_{Na_2O}(IV))] \end{aligned} \quad (9)$$

$$\begin{aligned}\Delta_f G^\circ(Na_3NbO_4(s)) = [&\Delta_f G^\circ(Na_2O(s)) + \Delta_f G^\circ(NaNbO_3(s)) \\ &+ RT\ln(a_{Na_2O}(V))] \end{aligned} \quad (10)$$

The roman numerals in the activity terms denote five two-phase regions where the pressure was measured in a temperature range of about 180 K. From the temperature dependence of $\Delta_f G^\circ$, it is possible to obtain the enthalpy and entropy of formation data according to:

$$\Delta_f H_T^\circ = -T^2\left[\frac{\partial(\Delta_f G_T^\circ/T)}{\partial T}\right]_p \quad (11)$$

and

$$\Delta_f S_T^\circ = \frac{\Delta_f H_T^\circ - \Delta_f G_T^\circ}{T} \quad (12)$$

respectively.

Until 1990 it was commonly accepted that during evaporation $Na_2O(g)$ decomposes to its elements in quite a high percentage so that the partial pressure of gaseous molecule $Na_2O(g)$ is very low and that the predominant species in the vapour are Na(g) and $O_2(g)$. Therefore vaporisation takes place as follows:

$$Na_2O(s) \Leftrightarrow Na_2O(g) \quad (13)$$

$$Na_2O(g) \Leftrightarrow 2Na(g) + 1/2O_2(g) \quad (14)$$

and the corresponding equilibrium constant of reaction (14) is

$$K_p(14) = \frac{p_{Na(g)}^2 p_{O_2(g)}^{1/2}}{p_{Na_2O(g)}} \quad (15)$$

Due to the congruency condition of (14) in a Knudsen cell the vapour pressure of O_2 can be expressed as [16], p. 40

$$P_{O_{2(g)}} = \frac{p_{Na(g)}}{4}\sqrt{\frac{M_{O_2}}{M_{Na}}} \quad (16)$$

and the vapour pressure of Na_2O can finally be expressed by

$$p_{Na_2O(g)} = \frac{p_{Na(g)}^{5/2}}{2K_p(24)}\left(\frac{M_{O_2}}{M_{Na}}\right)^{1/4} \quad (17)$$

The activity of Na_2O in a system is then obtained as:

$$a_{Na_2O} = \frac{p_{Na_2O(g)}}{p_{Na_2O(g)}^*} = \left(\frac{p_{Na(g)}}{p_{Na(g)}^*}\right)^{5/2} \quad (18)$$

Here, the symbol (*) represents pure Na_2O.

Thus, by measuring the equilibrium sodium vapour pressure in all neighbouring two-phase regions (Fig. 1), the standard Gibbs energies of formation for the individual compounds can be determined (Eqs. (6)–(10)), provided that $p_{Na(g)}^*$ is known with sufficient accuracy.

Steinberg and Schofield [17] cast doubt on accuracy of reaction (14) and propose the following process to govern the evaporation of sodium oxide:

$$2Na_2O(s) \Leftrightarrow 3Na(g) + NaO_2(g) \quad (19)$$

The reasoning behind this assumption is explained by the highly stable Na–O_2 bond (243 kJ/mol), determined by the authors in their flame experiments. The acceptance of thisprocess (29) would have

severe consequences for the interpretation of the mass spectrometric observations of Hildenbrand and Murad [18] and Brewer and Margrave [19], which are discussed by Steinberg and Schofield [17]. In the latter, the authors propose to re-calculate (examine) the former thermochemical data. In response, Hildenbrand and Lau [20] published an additional study on this subject, rejecting completely the postulate of Steinberg and Schofield [17]. Moreover, Soldan et al. [21] published *ab initio* calculations on the stability of the Na–O_2 bond (<160 kJ/mol), and found it to be much lower than that proposed by Steinberg and Schofield [17] indicating that the NaO_2(g) gaseous molecule cannot be the major species present in the vapour above solid Na_2O(s). The problem of detecting the NaO_2(g) molecule by mass spectrometry is that after ionisation, NaO_2^+ ions fragment into Na^+ ion and O_2 and only a minor portion of NaO_2^+ ions are detected by the mass spectrometer. The ionisation process of NaO_2 (g) can be described by:

$$\begin{aligned} NaO_2(g) + e^-(g) &= NaO_2{}^+(g) + 2e^-(g) \\ &= Na^+(g) + O_2(g) + 2e^-(g) \end{aligned} \quad (20)$$

The appearance energy of Na^+ ions by this process is certainly higher than the energy required to ionise sodium and the threshold of the process (20) could easily be detected in the ionisation curve of the sodium ion. However, the absence of any structure (*e.g.* breaking point) in the IE curve near the threshold can be regarded as a major proof for the absence of NaO_2(g) in the vapours over Na_2O(s). Such a proof was also presented by Hildenbrand and Lau [20] and confirmed in the present study (see Plot 1 in appendix). Notable is that some authors like Zaitzev et al. [22] use the idea of Steinberg and Schofield [17] to explain experimental evidences of their own. In the present work all calculations (Eqs. (6)–(10)), are based on the assumption that the processes (13) and (14) govern the evaporation and decomposition of Na_2O.

2. Instrumental

A common approach in KEMS experiments is to simultaneously evaporate the substance of interest with a standard material (under Knudsen conditions) from a Knudsen cell, positioned in front of the ion source of the mass spectrometer. The resultant narrow axial part of the effusing molecular and/or atomic beam enters the ionisation region where ions are created. Within the analyser the ions are then separated according to their mass-to-charge ratio and their abundance recorded by the detector. The vapour pressure is then obtained according to Eq. (21).

$$p_x = \left(\frac{\sum_i I_x^+}{\sum_i I_{\mathrm{ref}}}\right) \times \left(\frac{\sigma_{\mathrm{ref}}}{\sigma_x}\right) \times \left(\frac{\eta_{\mathrm{ref}}}{\eta_x}\right) \times p_{\mathrm{ref}} \quad (21)$$

Here p, σ, η and I refer to the pressures, ionisation cross-sections, isotope abundance factor and the ion currents of the reference material (ref) and the sample to be studied (x). If several kinds of ion species are generated during ionisation the total intensity of all the ions should be considered. Importantly, the reference material must not react or mix with the substance of interest and neither the reference nor the sample must interact with the material of the Knudsen cell. Typical pressures measured by KEMS are from 10^{-6} Pa up to few Pa, provided that Knudsen conditions are fulfilled *i.e.*, the mean free path of the molecules within the cell should be much greater than the orifice diameter. The temperature range of the measurements can be as high as 200 K, which is sufficient to reliably determine the Gibbs energy and enthalpy of the reactions to be studied.

2.1. Mass spectrometer and Knudsen evaporator

In this study a 60° magnetic low-resolution mass spectrometer with a modified Nier-type ion source was used. The exact instrumental details are published elsewhere [23] but importantly it has the ability to produce reliable ionisation efficiency curves several volts above the threshold region. The Knudsen cell embedded within a Mo crucible was placed in an alumina tube and heated resistively by a Mo wire (spiral). The heating zone must be sufficient to provide a minimal temperature gradient within both the Mo crucible and the Knudsen cell. The temperature was measured using a calibrated Ni/CrNi thermocouple point-welded onto the Mo crucible and maintained by a EUROTHERM programmable temperature controller accurate to ±1 K. Calibration was carried out by evaporation of known amount of silver through the knife edged orifice. Two layers of a tantalum radiation shield were then positioned around the Mo heating spiral to minimise heat loss and the thermal gradient. The distance from the cell orifice (Ø = 0.5 mm) to the entrance hole (Ø = 3 mm) and the centre of the ionisation chamber was 2 and 3 cm, respectively. A 5-mm-thick copper plate (with a circular 3 mm diameter opening) was then placed between the shutter plate and the ion source and cooled by liquid nitrogen. The plate allows most of the effusing materials to condense in order to prevent contamination of the ion source. In addition, the plate protects the source from the heat radiation emitted from the Knudsen evaporator. Between the plate and the tantalum radiation shields a manually operated shutter plate was installed to distinguish between the ions formed from background gases and those originating from the effusing molecules. In addition, to avoid contamination by oil from the rotary pumps penetrating the high vacuum, a helium Leybold cryo-pump was used that does not require a fore-pump. The detector part of the analyser tube was additionally evacuated using a turbo-molecular pump. Typical operating pressure in the ion source region and detector region was below 10^{-7} mbar.

Ions were then detected by an ETP active film electron multiplier (AF151H) operating in the counting mode using a 225 MHz HP 5315A counter. The multiplier was fed with −3.0 kV by a high voltage supply unit (FUG HCN 35 3500). The supply voltage was set so as to avoid mass discrimination on the first (conversion) dynode ('plateau' region). During measurements, when the shutter plate was closed, the counting rate was <10 s^{-1}, for all m/z of interest.

3. Materials and sample preparation

The powder samples were prepared by conventional solid state synthesis from high purity Nb_2O_5 (Sigma–Aldrich, 99.9%) and Na_2CO_3 (Sigma–Aldrich, 99.95–100.05%), which was high-energy milled prior to synthesis. Full details are published elsewhere [24] but in general powdered mixtures with different Na/Nb molar ratios (60/40, 40/60, 30/70, 15/85 and 5/95) were homogenised in a planetary ball mill (Fritsch Pulverisette 4 Vario-Mill) for 4 h, using acetone as the liquid medium. After drying the powders were pressed into pellets and calcined in closed alumina crucibles at 700 °C for 4–70 h. The pellets were subsequently crushed in an agate mortar and milled in a planetary ball mill for 4 h. The powders were then dried and used for Knudsen cell measurements.

For additional qualitative phase composition analysis, the as-synthesized powders were packed into platinum containers and heated at either 750 °C (60/40) or 900 °C (40/60, 30/70, 15/85 and 5/95) for 1 h. They were then quenched in liquid nitrogen to preserve the high-temperature phases, present during the KEMS measurement.

The X-ray diffraction (XRD) patterns were recorded within the angular 2θ range of 10–90°, using a 0.026° step and 100 s/step, on

Table 1
Values of "*A*" and "*B*" parameters and the pressure of sodium calculated for 1100 K for pure sodium oxide. Notice the significant difference between values of "*A*" and the resulting calculated pressure.

Author	Method	$-A$	B	Temperature range	p(Na)/Pa at T = 1100 K
Brewer and Margrave [19]	Mass loss	20180[a]	18.075[a]	918–1467 K	0.736[a]
Hildenbrand and Murad [18]	KEMS and calculated by authors from available thermodynamic data	30096	26.859	–	0.603
Piacente et al. [27]	Torsion effusion	27447	24.167	1150–1310 K	0.456
Hildenbrand and Lau [20]	Torsion effusion and KEMS	25894	23.055	980–1050 K	0.616
IVTANTHERMO	Calculated from IVTANTHERMO database [27]	29146	26.306	–	0.827
This work	KEMS	(28220 ± 1000)	(25.748 ± 0.2)	873 K – 1003 K	1.098 (±20%)

[a] Evaluated in this work from Brewer's mass loss data.

a PANalytical X'Pert PRO MPD diffractometer ($CuK_{\alpha 1}$ – Graphite monochromator). The phase composition of the samples was in agreement with the phase diagram in Fig. 1. However, according to Irle et al. [15] the $NaNb_3O_8$ phase is stable only above 677 °C, while our results indicate that this phase is present both in the quenched and slowly cooled samples.

For pressure measurements of Na(g) over pure Na_2O(s), Na_2O containing 12.16% Na_2O_2 (Alfa Aesar) was used. The as-received Na_2O was stored and loaded into the Knudsen cell under a dry atmosphere.

4. Experimental procedure and the results

A known weight of powdered samples (100 mg) together with pure silver (100 mg) was loaded into the alumina Knudsen cell. Silver served as a reference substance for the pressure calibration (internal calibration). After evacuation, the sample was heated at 10 K/min to 800 K. During this period only the ions belonging to CO_2 appeared in the mass spectra. After degassing (approx. 2 h) the temperature was increased at the same rate to 1000 K and then kept constant until the intensity of the Na^+ ion became constant. The time dependency (decreasing) of the intensity of Na^+ at the beginning of the experiment (see Plot 2 in appendix) indicates that the samples were not in complete thermodynamic equilibrium. It was also observed that the decreasing effect was dependent on the time elapsed between preparation and measurement. We believe that this effect is due to the trace amounts of hydrated samples (see text below). In some cases, such an effect was sustained for more than 50 h. Samples that had been stored for longer revealed a much more pronounced 'beginning decrease' and an extended time of equilibration. After this, the main equilibrium measurement could be started. This was performed by measuring the abundances of sodium and silver ions at the same temperature. Table I depicted in SI appendix shows a particular measurement of the measured composition in region III. Data of silver pressure were taken from Ref. [25]

From the measured pressure of Na(g), the activity of Na_2O was calculated using Eq. (22). It follows from Eq. (22) that pressure of a measured substance can be obtained from its ion intensity ratio versus reference. Moreover, if such ratio is measured also for pure Na_2O, the activity at temperature T can be obtained from double ratio as shown in Eq. (22),

$$a_{Na_2O} = \left[\frac{(I^+_{Na}/I^+_{Ag})}{(I^+_{Na}/I^+_{Ag})^*}\right]^{5/2}_T \tag{22}$$

free of most systematic errors. Ratio in denominator of Eq. (22) was obtained in separate experiment. It was accomplished by first heating (in the Knudsen cell) the as-received Na_2O(s) together with the internal standard (Ag) at 730 K in order to decompose substantial amount of Na_2O_2(s) contained in as-received Na_2O. The temperature was then slowly increased to 900 K to evaporate any sodium hydroxide, also present in the Na_2O(s); the process was monitored by following the decreasing abundances of Na_2OH^+(g) (m/z) = 63 and Na^+ ions (m/z = 23). Once the measured abundance was <10 counts/s (after 72 h) the equilibrium measurement was initiated. Details of this measurement are also given in Table II in appendix.

The symbol '*K*' in both tables denotes the sensitivity constant of the instrument and is defined as:

$$K = \left(\frac{p_{ref}}{\sum_i I_{ref}/\sigma_{ref}} \times \frac{1}{T}\right) \tag{23}$$

(see Eq. (21)), so that the measured pressure of sodium also shown in Tables I and II (appendix) is obtained as

$$p_{Na(g)} = K \times I^+_{Na} \times T \times \left(\frac{\sigma_{Ag}}{\sigma_{Na}}\right) \tag{24}$$

The ionisation cross-section of Na(g) and Ag(g) at 30 eV was taken from Lotz [26] as 3.12×10^{-16} cm^2 and 5.06×10^{-16} cm^2, respectively.

It should be noted here, that even not necessary our measured pressure of sodium over pure Na_2O is given in Table II (SI) for the sake of comparison with rather sparse experimental data.

Pressure of sodium over the Na_2O was first measured by Piacente et al. [27] and later on also by Hildenbrand and Lau [20] both using torsion effusion method, giving the enthalpy of evaporation significantly lower that could be evaluated from JANAF [28] and IVTANTHERMO [29] thermodynamic databases. In Table 1, all available literature data for the pressure of sodium over pure Na_2O(s) are shown, together with the results obtained from the present work. Data are given in a $\ln(p/\text{Pa}) = A/T + B$ format. Pressures are also shown in graphic form in Fig. 2.

It should be noted that the slope "*A*" directly correlates the reaction enthalpies (see Eqs. (30) and (34) The obtained value of (−28220 ± 1000) (depicted in Table 1) can be considered close to the true value since there is only a slight temperature drift in the instrumental sensitivity constant ('*K*') values observed in Tables I and II (SI). In other words, the measured temperature dependence (parameter '*A*') of the pressure of Ag agrees with the literature data proving the adequate operation of our mass spectrometer. In addition it is very close to the value (−29146) evaluated from IVTANTHERMO [29] database. Furthermore, the temperature range of our experiments are the largest of all present data and we were could measure at lower temperatures than the former researchers proving that the sensitivity of our technique (KEMS) was the highest.

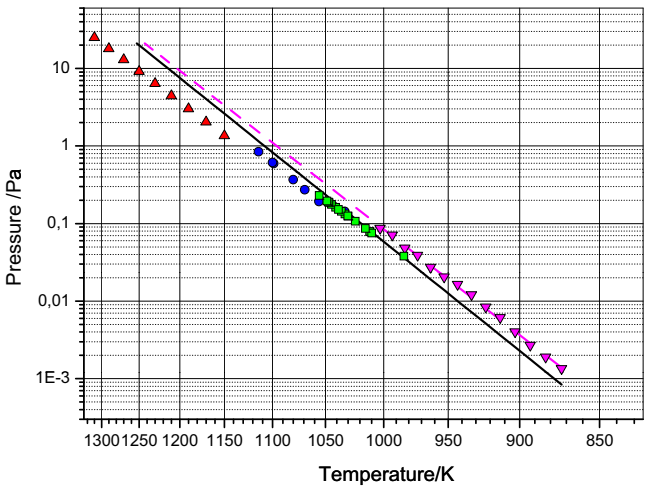

Fig. 2. Equilibrium pressure of sodium over pure solid Na_2O with varying temperature. Up triangles: Piacente et al. [27], circles: Hildenbrand and Murad [18], squares: Hildenbrand and Lau [20], solid line: calculated from IVTANTHERMO database [29], down-triangles: data points determined in this study, dashed line: calculated from the data points.

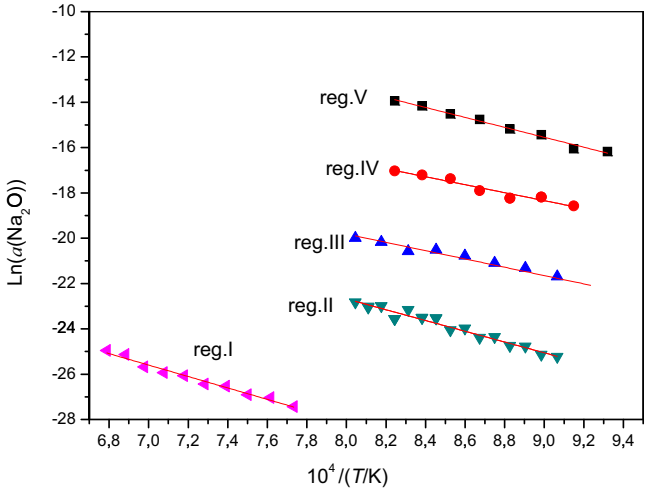

Fig. 3. Natural logarithm of sodium activity ln (a_{Na_2O}) in variation with $1/T$ in five solid two-phase regions.

For each composition in all regions several runs were measured with the reproducibility of the '*A*' value within ±1500. The selected measurements of Na_2O activity in all five regions are shown in Fig. 3.

Table 2 includes the parameters (*A* and *B*) of the measurements shown in Fig. 3, which allows the sodium oxide activity at various temperatures to be calculated for the assigned phase mixtures (regions).

The Gibbs energy of formation of $NaNb_{13}O_{33}(s)$ (Eq. (6)) from the component elements, as a function of temperature, can now be written as:

$$\Delta_f G_T^\circ(NaNb_{13}O_{33}(s)) = \frac{1}{2}\left[\Delta_f G_T^\circ(Na_2O(s)) + 13\Delta_f G_T^\circ(Nb_2O_5(s)) + RT\left(\frac{A_I}{T} + B_I\right)\right] \quad (25)$$

for which Gibbs energy of formation of solid $Na_2O(s)$ and $Nb_2O_5(s)$ from their elements, as a function of temperature, is needed. The data was obtained from IVTANTHERMO [29] in the form of:

$$\Delta_f G_T^\circ(Nb_2O_5(s)) = 1000(aT - b) \quad \text{and} \quad (26)$$

$$\Delta_f G_T^\circ(Na_2O(s)) = 1000(cT - d) \quad \text{both in kJ mol}^{-1} \quad (27)$$

Here *a*, *b*, *c* and *d* were obtained as 0.4086; 1867.1; 0.1358 and 411.65, respectively and Eq. (25) further becomes

$$\Delta_f G_T^\circ(NaNb_{13}O_{33}(s)) = \frac{1}{2}\left[13000(aT - b) + 1000(cT - d) + RT\left(\frac{A_I}{T} + B_I\right)\right] \quad (28)$$

Having expressed $\Delta_f G_T^\circ(NaNb_{13}O_{33})$ in analytical form one can obtain both $\Delta_f H_T^\circ(NaNb_{13}O_{33})$ and $\Delta_f S_T^\circ(NaNb_{13}O_{33})$ according to Eqs. (11) and (12).

Using Eq. (28) it is possible to evaluate the uncertainty resulting from the erroneous determination of parameters *A* and *B*. It is very small compared to the absolute value since the term that includes *A* and *B* is small (about 3%) when compared to the terms that include *a*, *b*, *c* and *d*. To obtain a more direct correlation between the measured parameters *A* and *B* and the thermodynamic functions it is better to calculate the formation of $NaNb_{13}O_{33}$ from the pure component oxides as follows:

$$\Delta_f G_T^\circ(ox)(NaNb_{13}O_{33}) = \frac{1}{2}R(A_I + B_I \cdot T) \quad (29)$$

$$\Delta_f H_T^\circ(ox)(NaNb_{13}O_{33}) = \frac{1}{2}R \cdot A_I \quad (30)$$

$$\Delta_f S_T^\circ(ox)(NaNb_{13}O_{33}) = -\frac{1}{2}R \cdot B_I \quad (31)$$

In this case, these functions directly correlate with the measured *A* and *B* and determine the solid state reaction (32)

$$1/2Na_2O(s) + 13/2Nb_2O_5(s) = NaNb_{13}O_{33}(s) \quad (32)$$

Once all three thermodynamic functions for $NaNb_{13}O_{33}$ have been obtained it is then possible to calculate all the others. Using $NaNbO_3(s)$ as an example, the Gibbs energy, enthalpy and entropy of formation from oxides is obtained as:

Table 2
Activities of sodium oxide in five two-phase regions in the form of ln $(a_{Na_2O}) = A/T + B$ and values calculated at 1000 K.

Region	Phases present	Interval of measurement/K	$\ln(a_{Na_2O}) = A/T + B$		a_{Na_2O} at 1000 K
			A (±1500)	*B* (±0.3)	(±40%)
I	$Nb_2O_5 + NaNb_{13}O_{33}$	1273–1473	−25200	−7.93	3.9E−15
II	$NaNb_{13}O_{33} + NaNb_3O_8$	1113–1243	−23800	−3.64	1.2E−12
III	$NaNb_3O_8 + Na_2Nb_4O_{11}$	1083–1243	−15900	−7.15	9.4E−11
IV	$Na_2Nb_4O_{11} + NaNbO_3$	1073–1233	−17600	−2.52	1.9E−9
V	$NaNbO_3 + Na_3NbO_4$	1073–1213	−21900	4.19	2.0E−8

Table 3
Gibbs energy of formation determined from elements and from oxides as a function of temperature. The accepted equations for $\Delta_f G_T^\circ$(el) (third column) were obtained directly from measured $\Delta_f G_T^\circ$(ox) and corrected $\Delta_f H^o$(ox) (last column in Table 4).

Compound	$\Delta_f G_T^\circ$(ox) (kJ/mol)	$\Delta_f G_T^\circ$(el) (kJ/mol)	$\Delta_f G_T^\circ$(el) (accepted)(kJ/mol)	$\Delta_f G_T^\circ$(el) (Amin [7]) (kJ/mol)
$NaNb_{13}O_{33}$	$-0.03297T - 104.9$	$2.690T - 12450$	$2.692T - 12448$	–
$NaNb_3O_8$	$-0.01925T - 100.3$	$0.660T - 3105$	$0.652T - 3098$	$0.789T - 3347.3$
$Na_2Nb_4O_{11}$	$-0.04548T - 177.9$	$0.905T - 4321$	$0.909T - 4326$	$1.082T - 4664.2$
$NaNbO_3$	$-0.01660T - 81.0$	$0.256T - 1220$	$0.263T - 1227$	$0.279T - 1317.0$
Na_3NbO_4	$0.01822T - 263.3$	$0.425T - 1813$	$0.425T - 1813$	$0.272T - 1751.6$

Table 4
Heat of formation, Gibbs energy of formation and entropy of formation at 1000 K, from elements and from oxides. Also shown are the "corrected" values for $\Delta_f H^\circ$(ox) assuming constant partial enthalpies over a broad composition interval. Values in brackets are the corrected $\Delta_f S_{1000\,K}^\circ$(ox) data obtained from corrected $\Delta_f H^\circ$(ox) and measured $\Delta_f G_T^\circ$(ox).

Compound	$\Delta_f H^\circ$(el) (kJ/mol)	$\Delta_f G_{1000\,K}^\circ$(el) (kJ/mol)	$\Delta_f H^\circ$(ox) (kJ/mol)	$\Delta_f G_{1000\,K}^\circ$(ox) (kJ/mol)	$\Delta_f S_{1000\,K}^\circ$(ox) (J mol^{-1} K^{-1})	$S_{1000\,K}^\circ$ (J mol^{-1} K^{-1})	$\Delta_f H^\circ$(ox) (corr.) (kJ/mol)
$NaNb_{13}O_{33}$	−12447	−9756	−105 (±10)	−138 (±15)	33 (32) (±5)	2305	−106 (±10)
$NaNb_3O_8$	−3107	−2445	−100 (±10)	−120 (±15)	19 (29) (±5)	611	−91 (±10)
$Na_2Nb_4O_{11}$	−4324	−3416	−178 (±10)	−223 (±15)	45 (43) (±5)	893	−180 (±10)
$NaNbO_3$	−1220	−965	−81 (±10)	−98 (±15)	17 (10) (±5)	272	−88 (±10)
Na_3NbO_4	−1814	−1388	−263 (±10)	−245 (±15)	−18 (−17)(±5)	412	−262 (±10)

$$\Delta_f G_T^\circ(\mathrm{ox})(NaNbO_3(s)) = -R\left[\left(\frac{1}{26}(A_I - T\cdot B_I) - \frac{5}{39}(A_{II} + T\cdot B_{II}) - \frac{1}{12}(A_{III} + T\cdot B_{III}) - \frac{1}{4}(A_{IV} + T\cdot B_{IV})\right)\right] \quad (33)$$

$$\Delta_f H_T^\circ(\mathrm{ox})(NaNbO_3(s)) = R\left(\frac{1}{26}A_I + \frac{5}{39}A_{II} + \frac{1}{12}A_{III} + \frac{1}{4}A_{IV}\right) \quad (34)$$

$$\Delta_f S_T^\circ(\mathrm{ox})(NaNbO_3(s)) = -R\left(\frac{1}{26}B_I + \frac{5}{39}B_{II} + \frac{1}{12}B_{III} + \frac{1}{4}B_{IV}\right) \quad (35)$$

Here the subscripts represent the measured composition regions in the phase diagram and numerals are the stoichiometric factors. The results are shown in Tables 3 and 4.

The results in the first column of Table 3 are considered as "primary" data, obtained directly from KEMS measurements without using data from the literature. Fig. 4 gives a graphic representation of the "primary" data at 1000 K. All other functions, $\Delta_f H^\circ$(el), $\Delta_f G_T^\circ$(el) and S_T°, contained in Tables 3 and 4 were obtained using both "primary" and literature data. The accepted values of $\Delta_f G_T^\circ$(el) (third column of Table 3) were obtained from directly measured $\Delta_f G_T^\circ$(ox), corrected $\Delta_f H^\circ$(ox) (seventh column of Table 4 and literature $\Delta_f G_T^\circ$(el) values of Na_2O and Nb_2O_5) using basic thermodynamic relations.

The differences in Amin's [7] values for $\Delta_f G_T^\circ$(el) and this study's results shown in Table 3 do need an explanation. Amin's results for $\Delta_f G_T^\circ$(el) of individual phases are based on the estimated value for $\Delta_f H^\circ$(el) of $NaNbO_3$(s) by Lindemer et al. [12] followed by Uhlich's [30] first approximation to obtain $\Delta_f G_T^\circ$(el) for this compound. Our results however are obtained directly *i.e.*, from the measured parameters *A* and *B* and the well-defined thermodynamic functions of Na_2O(s) and Nb_2O_5(s), avoiding the systematic errors introduced by Lindemer's estimations of $\Delta_f H^\circ$(el).

The Gibbs energy, enthalpy and entropy of formation data of the mixed oxide compounds correspond to 1 mol of the given formula in Tables 3 and 4 where the total amount of oxides vary: *e.g.* $NaNbO_3$(s) is formed from 1 mol oxide (1/2 mol Na_2O and 1/2 mol Nb_2O_5) whereas $NaNb_{13}O_{33}$ is formed from 7 mol oxide (1/2 mol Na_2O and 13/2 mol Nb_2O_5). Nevertheless, it is worth to express the molar thermodynamic quantities of mixing or formation (per 1 mol of total number of mixed oxide). Fig. 4 presents the molar (per 1 mol of oxide) Gibbs energy, enthalpy and entropy of formation for the mixed oxides, formed from the pure component oxides, as a function of composition.

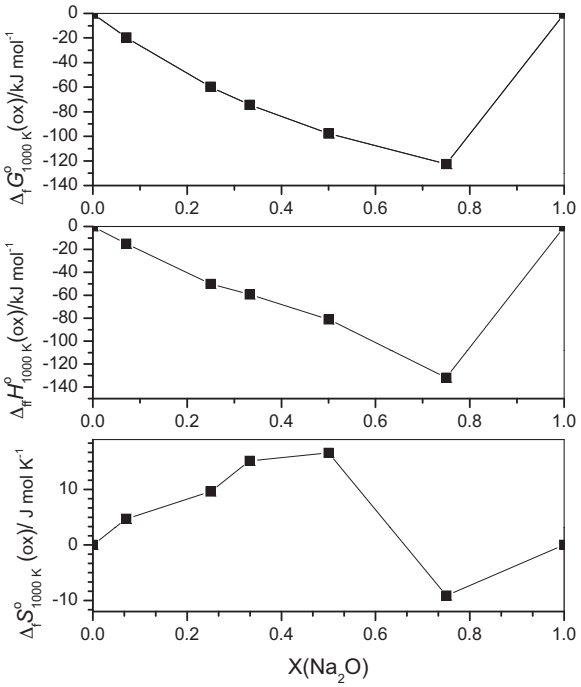

Fig. 4. Molar (per 1 mol of oxide) Gibbs energy, enthalpy and entropy of formation of the mixed oxide compounds formed from the pure component oxides as a function of composition.

The seemingly linear relation between $\Delta_f H^\circ$(ox) and mole fraction of Na_2O observed in Fig. 4 justify a regression to be performed on the $\Delta_f H^\circ$(ox) data and to obtain the partial enthalpies of formation for Na_2O and Nb_2O_5, which are −174(±15) kJ/mol and −2.9(±0.3) kJ/mol, respectively. This large difference in the two partial enthalpies of formation values makes the integral enthalpy of formation *vs.* composition function ($\Delta_f H^\circ$(ox) *vs.* *X*) linear in a quite a broad composition range. In Fig. 5 the measured (per formula) $\Delta_f H^\circ$(ox) data are correlated with the 'corrected' values for all five compounds. We call the latter data as "corrected" values for $\Delta_f H^\circ$(ox). By mathematical cross examination of the effect of "*A*" and "*B*" values on $\Delta_f H^\circ$(ox), $\Delta_f G_T^\circ$(ox) and $\Delta_f S_T^\circ$(ox) we found that specified uncertainty in "*A*" and "*B*" results in errors of about ±10 kJ/mol, ±15 kJ/mol and ±3 J mol^{-1} K^{-1}, respectively.

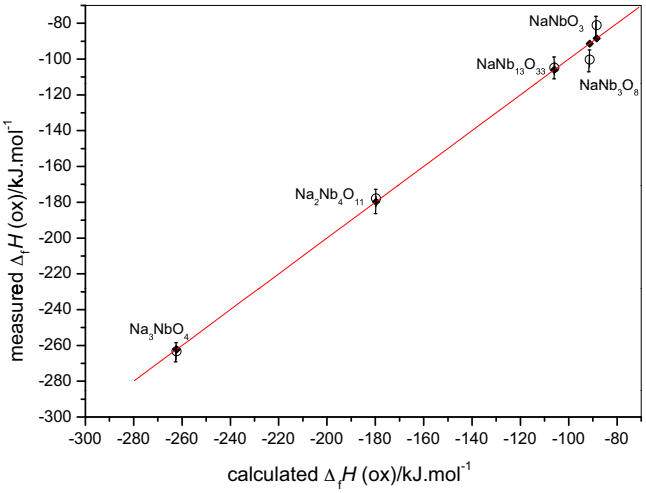

Fig. 5. Measured and calculated *vs.* calculated molar (per 1 mol of given chemical formula in Table 4) enthalpy of formation of the mixed oxide compounds formed from the pure component oxides. Full squares: calculated (improved) values, Open circles: measured values.

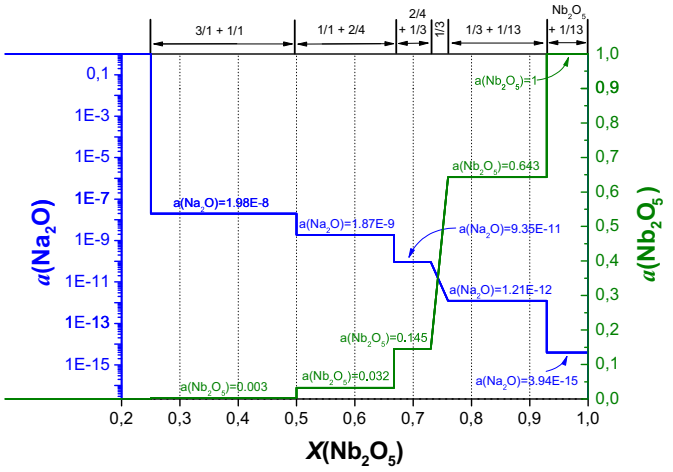

Fig. 6. Activities of Nb_2O_5 and Na_2O at 1000 K in various solid two-phase regions.

For Na_3NbO_4 the calculated heat of formation from pure oxides becomes

3/2(−173.9) kJ/mol + 1/2(−2.92) kJ/mol = −262 kJ/mol, while the measured result is −263 kJ/mol (Table 4).

A similar linearization approach is used by Moiseev et al. [31] for a series of 11 compounds of the $SrO + Bi_2O_3$ system. From the number of measured data, authors deduced an empirical relation between standard heat of formation of complex oxide and the number of oxygen atoms in complex oxide as:

$$\Delta_f H^\circ(\text{ox})/\text{kJ/mol} = (-16.048 \pm 5.145) \times n_{(O)} \quad (36)$$

where $n_{(o)}$ is the number of oxygen atoms in a given complex oxide.

It should be mentioned, that such linearization implicitly assumes similar and constant partial enthalpies over a broad concentration range which needs to be verified experimentally. In the present case such evidence exists but still, Eq. (36) fails in present case due to the noticeable differences in partial enthalpies.

The first column in Table 5 shows the calculated standard absolute entropies obtained on the basis of our measured $\Delta_f S_T^\circ(\text{ox})$ values and the $C_p(T)$ values of $Na_2O(s)$ and $Nb_2O_5(s)$ obtained from the IVTANTHERMO [29] database using the Neumann–Kopp's rule. Certainly, these values should be considered as rough approximations since, with the exception of $NaNbO_3(s)$, the experimental heat capacities of the compounds in question are still missing. The second column presents the corresponding values obtained using a similar procedure as used for the enthalpies of formation, by regression. In this case the coefficients of regression are 80.37(±5) J mol^{-1} K^{-1} and 152.8(±10) J mol^{-1} K^{-1} for Na_2O and Nb_2O_5, respectively. It should be noted, that the standard entropy values for $NaNbO_3$ and Na_3NbO_4 at 298 K are close to Lindemer et al.'s [12] estimations of 116.3 J mol^{-1} K^{-1} and 192.8 J mol^{-1} K^{-1}. Moreover, the low temperature heat capacity of the single-crystalline $NaNbO_3(s)$ was measured between 4 K and 290 K by Drulis and Konieczny [32]. We used their $C_p(T)$ data to calculate $S_{298\,K}$ as 114 J mol^{-1} K^{-1}. This value can be considered as the first experimental value for the standard entropy of $NaNbO_3$ matching closely our estimated value.

From the measured Na_2O activity data, the activity data of Nb_2O_5 using the Gibbs–Duhem (GD) integration (at T = 1100 K) were determined and are presented in Fig. 6. Please note, that the activity over the slightly broader solid solution (mono-phase) region of $NaNb_3O_8$ was not measured. For that reason, the activity drop across this region is drawn symbolically as linear. Nevertheless, this region is not broad enough to have a significant effect on the Nb_2O_5 activity data obtained by GD integration so that the GD integration area in this region is negligible. Therefore the linear approximation of the activity *vs.* composition function over this mono-phase region was sufficient.

4.1. Reliability of the results and sources of errors

As previously mentioned, the reliability of the measured sodium pressure and its temperature dependence are the two most relevant factors affecting the final results. First, a 40% error in pressure (which is usual in KEMS) results in a 100% error in activity (see Eq. (18)), which causes only a slight error in $\Delta_f G_T^\circ(\text{el})$ of about ±3 kJ/mol. A typical error in determining the slopes (parameters A) is about ±1500, which makes the uncertainty in enthalpy ±6 kJ/mol (see Eq. (30)) for the first region. For all subsequent regions this error accumulates in some way as can be concluded from Eq. (34), which leads to the scattering of results in the measured enthalpies.

From Fig. 5 and the agreement between measured and calculated $\Delta_f H^\circ$ (Table 4), it can be seen that all parameters 'A' are self-consistent. Finally, since $\Delta_f S_T^\circ(\text{ox}) = (\Delta_f H_T^\circ(\text{ox}) - \Delta_f G_T^\circ(\text{ox}))/T$, values shown in Table 4, can also be considered close to the real values. However, the formation enthalpy of $NaNbO_3$

Table 5
Standard entropy of compounds calculated from the measured $\Delta_f S_{1000\,K}^\circ(\text{ox})$ values and $C_p(T)$ functions. The Neumann–Kopp's additivity rule was used for this purpose.

Compound	Obtained $S_{298\,K}^\circ$ (J mol^{-1} K^{-1})	Estimated $S_{298\,K}^\circ$ (J mol^{-1} K^{-1})	Lindemer et al.'s [12] estimation of $S_{298\,K}^\circ$ (J mol^{-1} K^{-1})	Calculated by us from low temperature Cp(T) data Ref. [32] (J mol^{-1} K^{-1})
$NaNb_{13}O_{33}$	1023	1033	–	–
$NaNb_3O_8$	278	269	–	–
$Na_2Nb_4O_{11}$	417	385	–	–
$NaNbO_3$	129	116	116.3	114
Na_3NbO_4	173	196	192.8	–

from oxides has been measured by Pozdnyakova and Navrotsky [8] using drop solution calorimetry. The resultant value of −153 kJ/mol is higher than our measured of −81.02 kJ/mol (consider Eq. (34)). To match the result from this study to those reported in the literature it is necessary to increase measured slopes (parameters A) by a factor of two. However, the corresponding slopes reported in Ref. [7] (obtained by electrochemical solid electrolyte galvanic cell approach) are similar to this study's, which confirms the reliability of our slopes. Thus, the value of −153 kJ/mol of Pozdnyakova and Navrotsky [8] seems to be too high.

4.2. Equilibrium calculations

To test the reliability of thermodynamical functions obtained within this work, we incorporated them into the IVTANTHERMO EQUI-CALC32 program in order to perform various equilibrium calculations. Table III (SI) gives all the necessary data, which were incorporated into the program.

The origin of data in Table III (SI) is self evident from the text above except for the enthalpy increment values, which were an approximation derived from Eq. (37), as follows:

$$(H_{298\ \mathrm{K}}{}^{\circ} - H_{0\ \mathrm{K}}{}^{\circ}) = 216 S_{298\ \mathrm{K}}{}^{\circ} \exp\left(\frac{S_{298\ \mathrm{K}}{}^{\circ}/n}{17}\right) \quad \text{in cal mol}^{-1} \quad (37)$$

where "n" is the number of atoms in one molecule of the compound (Ref. [31]). It is worth noting, that the calculated enthalpy increment of $NaNbO_3$ agrees with the measured value of Drulis and Konieczny [32]. For the sake of consistency an approximate value of $C_{p298\ \mathrm{K}}$ ($NaNbO_3$(s)) is used rather than the more reliably measured value of 110 J mol^{-1} K^{-1} Ref. [32].

The simulated equilibrium results of the solid phase and the gaseous phase composition of the mechanical mixture of 0.9 mol of Na_3NbO_4 and 0.1 mol of $NaNb_3O_8$ at 1250 K in air at 1 bar are depicted in Appendix. As expected from the phase diagram these two compounds react to produce 0.4 mol of $NaNbO_3$ and 0.8 mol of Na_3NbO_4 according to Eq. (38)

$$0.9Na_3NbO_4(s) + 0.1NaNb_3O_8(s) = 0.4NaNbO_3(s) + 0.8Na_3NbO_4(s) \quad (38)$$

The change in Gibbs energy for this reaction is −2.6 kJ/mol which can be calculated by using the values (accepted values of $\Delta_f G_T{}^{\circ}$(el)) given in Table 3. The resulting equilibrium solid phase composition corresponds to region V in which only $NaNbO_3$(s) and Na_3NbO_4(s) solid compounds coexist at a specified temperature, according to phase diagram. One can also observe that the most relevant sodium containing gaseous species are $NaNO_3$(g) and $NaNO_2$(g) with comparable amounts and/or pressures, which can be calculated from the data shown in data sheet in Appendix. Similar calculations were performed between 1000 K and 1400 K in an air, argon and a pure oxygen atmosphere (Fig. 7). Evidently, sodium nitrate and nitrite are the dominant sodium containing species in the vapour phase if thermodynamic equilibrium is attained. In 1956 Freeman [33] reported his kinetic observations of the thermal decomposition of sodium nitrate. According to his measurements $NaNO_3$ readily decomposes at temperatures above 900 °C to form N_2, O_2, minor amounts of NO, and a solid residue, believed to be Na_2O. Our present EQUI-CALC32 calculation performed at 1273 K confirms decomposition of $NaNO_3$ to the same gaseous species with the addition of gaseous $NaNO_3$, $NaNO_2$ and a condensed residue of Na_2O_2. In any case, as far as the sodium loss during heat treatment of sodium niobate is concerned, an oxygen atmosphere is more suitable than atmospheric air for two reasons. First, in pure oxygen only sodium gas can be formed, and second, its concentration is essentially reduced by a high concentration of oxygen.

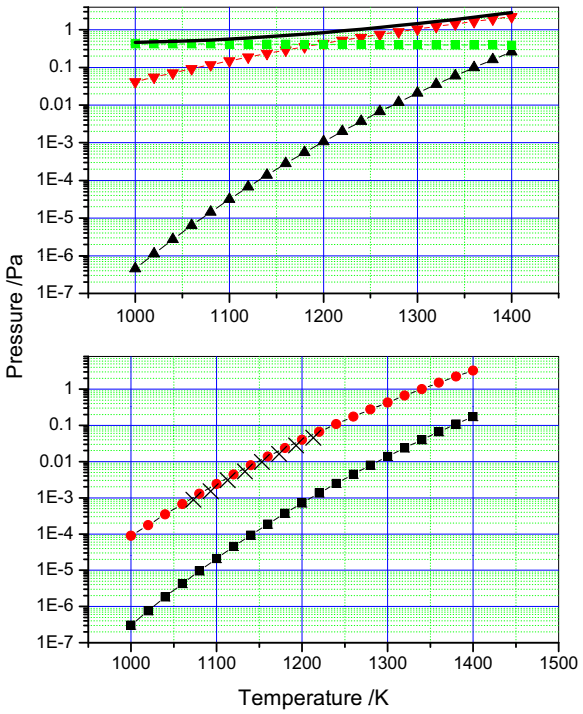

Fig. 7. Top calculated equilibrium pressures of vapour species over $Na_3NbO_4 + NaNbO_3$ in air. Up triangles = Na, down triangles = $NaNO_3$, squares = $NaNO_2$ and solid line = total pressure. Bottom: calculated equilibrium pressures of sodium over the $Na_3NbO_4 + NaNbO_3$ in: squares = pure oxygen, circles = argon and crosses = measured points.

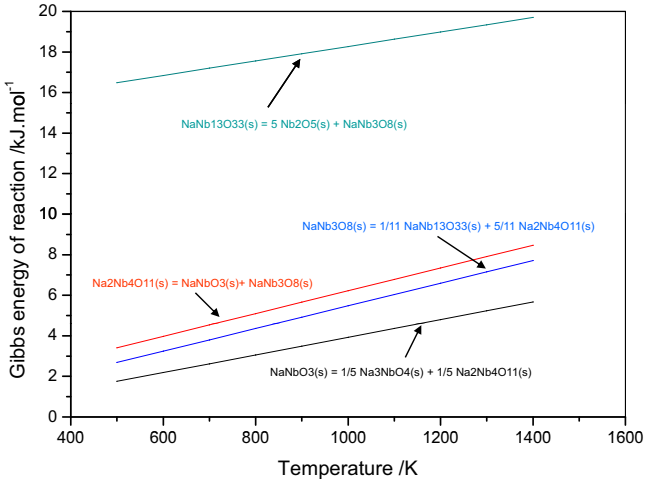

Fig. 8. Molar Gibbs energy of decomposition reaction of individual phases (compounds) to their neighbouring phases with temperature. Note that $NaNb_3O_8$ seems to be stable also below 670 °C.

Fig. 8 presents Gibbs energy of decomposition of investigated compounds (phases) to their neighbouring phases. The stability of all phases slightly increases with temperature. Note also that $NaNb_3O_8$ seems to be stable also at lower temperatures than those proposed by Ref. [15] (see also Fig. 1).

5. Conclusions

1. From the measured equilibrium pressures of Na(g) over selected Na_2O–Nb_2O_5 mixtures the Gibbs energy of formation of Na_3NbO_4, $NaNbO_3$, $Na_2Nb_4O_{11}$, $NaNb_3O_8$ and $NaNb_{13}O_{33}$ solid

compounds from their pure component oxides were determined.

2. From the temperature dependences of standard Gibbs energies of formation the standard enthalpies and entropies of formation of these mixed oxide compounds were obtained from both the pure component oxides and from elements. The partial enthalpies of formation of the mixed oxides from their pure component oxides were found very different and surprisingly constant over a broad composition interval, *i.e.*, $-174(\pm15)$ kJ/mol and $-2.9(\pm0.3)$ kJ/mol for Na_2O and Nb_2O_5, respectively. Thus, heat of formation of any compound in this system mostly depends on quantity of sodium oxide.
3. From the measured $\Delta_f S_T^\circ(\mathrm{ox})$ and estimated $C_p(T)$ data of the oxide compounds, the standard absolute entropies were evaluated as a rough estimation. Thus, we believe that the "estimated" values (Table 5) are more realistic. In particular, the estimated standard entropy of $NaNbO_3$ agrees with the experimental value we obtained from the measured $C_p(T)$ data of $NaNbO_3$ data provided in the literature. Also, our estimated $S_{298\,K}^\circ$ of Na_3NbO_4 and $NaNbO_3$ are both close to the values estimated by Lindemer et al. [12] as 192.8 J mol^{-1} K^{-1} and 116.3 J mol^{-1} K^{-1}, respectively.
4. Supplementing the EQUI-CALC 32 IVTANTHERMO database program with data provided by this work it was possible to reproduce the measured activities in regions III, IV and V rather well. The calculated composition of the gaseous phase indicates that the formation of sodium nitrate and sodium nitrite during the heat treatment of $NaNbO_3$ in air is thermodynamically possible, being the predominant sodium containing species during evaporation. However more accurate equilibrium results will be possible when the measured $C_p(T)$ and the $(H_{298\,K} - H_{0\,K})$ enthalpy increment values become available for all mixed oxide compounds.
5. Using our accepted values of $\Delta_f G_T^\circ(\mathrm{el})$, $NaNb_3O_8(s)$ seems to be stable against decomposition to $(Na_2Nb_4O_{11}(s)$ and $Nb_2O_5(s)$ also below 677 °C. This was confirmed by X-ray analysis of the unquenched sample Na/Nb = 30/70 within the framework of the present investigation.

Acknowledgment

This work was supported by the Slovenian Research Agency (1000-08-310121; P2-0105; J2-1227).

Appendix A. Supplementary data

Supplementary data associated with this article can be found, in the online version, at doi:10.1016/j.ijms.2011.08.028.

References

[1] J. Rödel, W. Jo, K.T.P. Seifert, E.-M. Anton, T. Granzow, D. Damjanovic, Perspective on the development of lead-free piezoceramics, J. Am. Ceram. Soc. 92 (6) (2009) 1153–1177.
[2] T.R. Shrout, S.J. Zhang, Lead-free piezoelectric ceramics: alternatives for PZT? J. Electroceram. 19 (2007) 111–124.
[3] B. Malič, A. Benčan, T. Rojac, M. Kosec, Lead-free piezoelectrics based on alkaline niobates: synthesis, sintering and microstructure, Acta Chim. Slov. 55 (2008) 719–726.
[4] Y. Saito, H. Takao, T. Tani, T. Nonoyama, K. Takatori, T. Homma, T. Nagaya, M. Nakamura, Lead-free piezoceramics, Nature 432 (2004) 84–87.
[5] P. Sue, Contribution a l'etude des niobates, Ann. Chim. 7 (1937) 493–592.
[6] H. Näfe, R. Amin, F. Aldinger, Thermodynamic characterisation of the eutectic phase mixture $NaNbO_3/Na_3NbO_4$ part I: literature survey, J. Am. Ceram. Soc. 90 (2007) 3224–3226.
[7] R. Amin, Solid state electrochemical characterization of thermodynamical properties of sodium–oxygen metal systems, PhD Thesis, University of Stuttgart, 2005.
[8] I. Pozdnyakova, A. Navrotsky, Thermodynamic and structural properties of sodium lithium niobate solid solutions, J. Am. Ceram. Soc. 85 (2) (2002) 379–384.
[9] H. Xu, A. Navrotsky, Y. Su, M.L. Balmer, Perovskite solid solutions along the $NaNbO_3$–$SrTiO_3$ join: phase transitions, formation enthalpies and implications for general perovskite energetic, Chem. Mater. 17 (2005) 1880–1886.
[10] A. Shigemi, T. Wada, Enthalpy of formation of various phases and formation energy of point defects in perovskite-type $NaNbO_3$ by first principles calculation, Jpn. J. Appl. Phys. 43 (2004) 6793–6798.
[11] N.K. Vaskresenskaya, G.P. Budova, Approximate calculation of the heats of formation of lithium, sodium and potassium metaniobates, Russ. J. Inorg. Chem. 14 (1969) 1566–1567.
[12] T.B. Lindemer, T.M. Besman, C.E. Jonson, Thermodynamic review and calculations—alkali-metal oxide systems with nuclear fuels, fission products and structural materials, J. Nucl. Mater. 100 (1981) 178–226.
[13] V.S. Yungman (Ed.), Thermal Constants of Substances, Begell House Inc./John Wiley & Sons Inc., N.Y., 1999.
[14] M.W. Shafer, R. Roy, Phase equilibria in the system Na_2O–Nb_2O_5, J. Am. Ceram. Soc. 42 (10) (1959) 482–486.
[15] E. Irle, R. Blachnik, B. Gather, The phase diagrams of Na_2O and K_2O with Nb_2O_5 and the ternary system Nb_2O_5–Na_2O–Yb_2O_3, Thermochim. Acta 179 (1991) 157–169.
[16] V.L. Stolyarova, G.A. Semenov, Mass spectrometric study of the vaporization of oxide systems, 1st ed., John Wiley & Sons, 1994.
[17] M. Steinberg, K. Schofield, A re-evaluation of the vaporisation behaviour of sodium oxide and bond strength of NaO and Na_2O: implications for the mass spectrometric analyses of alkali/oxygen systems, J. Chem. Phys. 94 (5) (1991) 3901–3907.
[18] D.L. Hildenbrand, E. Murad, Dissociation of NaO(g) and the heat of atomisation of Na_2O(g), J. Chem. Phys. 53 (9) (1970) 3403–3408.
[19] L. Brewer, J. Margrave, The vapour pressure of lithium and sodium oxides, J. Phys. Chem. 59 (1955) 421–425.
[20] D.L. Hildenbrand, K.H. Lau, Mass spectrum and sublimation pressure of sodium oxide vapour: stability of the superoxide molecule NaO_2, J. Chem. Phys. 98 (5) (1993) 4076–4081.
[21] P. Soldan, E.P.F. Lee, S.D. Gamblin, T.G. Wright, Na_2O and Na_2O^+ thermodynamics and low electronic states, J. Phys. Chem. A 104 (15) (2000) 3317–3325.
[22] A.I. Zaitzev, N.E. Shelkova, B.M. Mogutnov, Thermodynamics of Na_2O–SiO_2 melts, Inorg. Mater. 36 (6) (2000) 529.
[23] A. Popovic, Mass spectrometric determination of the cross-sections of BaO, Ba, BaF_2 and BaI_2 by electron impact, Int. J. Mass Spectrom. 230 (2003) 99–112.
[24] J. Koruza, J. Tellier, B. Malič, V. Bobnar, M. Kosec, Phase transitions of sodium niobate powder and ceramics, prepared by solid state synthesis, J. Appl. Phys. 108 (11) (2010) 113509.
[25] J.L. Margrave (Ed.), The Characterization of High-Temperature Vapors, John Wiley, N.Y., 1967.
[26] J. Drowart, C. Chatillon, J. Hastie, D. Bonnell, High temperature mass spectrometry: accuracy of the method and influence of the ionisation cross sections, Pure Appl. Chem. 77 (4) (2005) 683 (IUPAC Technical Report).
[27] V. Piacente, A. Desideri, G. Bardi, Torsion effusion of sodium partial pressure over Na_2O, J. Electrochem. Soc. 119 (1972) 75–76.
[28] M.W. Chase, NIST-JANAF Themochemical Tables, J. Phys. Chem. Ref. Data. Monograph 9, fourth ed., 1998.
[29] IVTANTHERMO, Glushko Thermocenter of RAS, Database on Thermodynamic Properties of Individual Substances and Thermodynamic modelling Software 1992–2000.
[30] O. Kubaschewski, C.B. Alcock, Metallurgical Thermochemistry, fifth ed., Pergamon press, N.Y., 1979.
[31] G. Moiseev, N. Zaiblikova, V. Jzukovski, S. Zaitzeva, N.Y. Ilynych, J. Šestak, Thermochemical and thermodynamical properties of 14 complex oxides in the SrO–Bi_2O_3 system, Thermochim. Acta 282/283 (1996) 191–204.
[32] M. Drulis, K. Konieczny, Low-temperature heat capacity of $NaNbO_3$ compound, Mater. Sci. Eng. B72 (2000) 19–22.
[33] E.S. Freeman, The kinetics of the thermal decomposition of sodium nitrate and of the reaction between sodium nitrite and oxygen, J. Phys. Chem. 60 (11) (1956) 1487–1493.